Science Bulletin

Future biomass carbon sequestration capacity of Chinese forests

Yitong Yao, Shilong Piao and Tao Wang

Citation: Science Bulletin **63**, 1108 (2018); doi: 10.1016/j.scib.2018.07.015

View online: http://engine.scichina.com/doi/10.1016/j.scib.2018.07.015

View Table of Contents: http://engine.scichina.com/publisher/scp/journal/SB/63/17

Published by the Science China Press

Science Bulletin 63 (2018) 1108–1117

Contents lists available at ScienceDirect

Science Bulletin

journal homepage: www.elsevier.com/locate/scib

Article

Future biomass carbon sequestration capacity of Chinese forests

Yitong Yao [a], Shilong Piao [a,b,c,*], Tao Wang [b,c]

[a] Sino-French Institute for Earth System Science, College of Urban and Environmental Sciences, Peking University, Beijing 100871, China
[b] Key Laboratory of Alpine Ecology and Biodiversity, Institute of Tibetan Plateau Research, Chinese Academy of Sciences, Beijing 100085, China
[c] Center for Excellence in Tibetan Earth Science, Chinese Academy of Sciences, Beijing 100085, China

ARTICLE INFO

Article history:
Received 10 March 2018
Received in revised form 6 July 2018
Accepted 9 July 2018
Available online 24 July 2018

Keywords:
Forest biomass
Carbon sequestration
Forest age
Climate change
Rising CO_2 concentration

ABSTRACT

Chinese forests, characterized by relatively young stand age, represent a significant biomass carbon (C) sink over the past several decades. Nevertheless, it is unclear how forest biomass C sequestration capacity in China will evolve as forest age, climate and atmospheric CO_2 concentration change continuously. Here, we present a semi-empirical model that incorporates forest age and climatic factors for each forest type to estimate the effects of forest age and climate change on total forest biomass, under three different scenarios based on the fifth phase of the Coupled Model Intercomparison Project (CMIP5). We estimate that age-related forest biomass C sequestration to be 6.69 Pg C (~0.17 Pg C a^{-1}) from the 2000s to the 2040s. Climate change induces a rather weak increase in total forest biomass C sequestration (0.52–0.60 Pg C by the 2040s). We show that rising CO_2 concentrations could further increase the total forest biomass C sequestration by 1.68–3.12 Pg C in the 2040s across all three scenarios. Overall, the total forest biomass in China would increase by 8.89–10.37 Pg C by the end of 2040s. Our findings highlight the benefits of Chinese afforestation programs, continued climate change and increasing CO_2 concentration in sustaining the forest biomass C sink in the near future, and could therefore be useful for designing more realistic climate change mitigation policies such as continuous forestation programs and careful choice of tree species.

1. Introduction

The biomass carbon (C) sequestration capacity of forests is of great interest for mitigation of global warming [1–3], given that forests store about 45% of the C in the terrestrial biosphere [4] and their C uptake could effectively and economically offset fossil fuel C emissions [5–8]. Much knowledge has been acquired about the forest C cycle [1,9,10], but large gaps still remain. One particular area of uncertainty is the estimation of forest biomass C sequestration capacity in the near future in China. Large-scale afforestation and reforestation programs have been implemented in China since the 1970s [11], and China now has a larger area of plantation forest than any other country [12]. According to the 8th Chinese forest inventory statistics [12], the percentage of forest cover has steadily increased from 12.70% in the early 1970s to 21.63% in 2009–2013. These forests are characterized by young forest age structures and relatively low biomass C density [2,13–15]. For example, the mean forest age in China was estimated to be ~40 years in the 2000s [16] and the mean forest biomass C density recorded in the latest national inventory statistics was <50 Mg C ha^{-1} [14]. These values are much lower than those for forests at similar latitudes in the United States where the aboveground biomass C density is ~88 Mg C ha^{-1} [17,18]. This characteristic young forest age structure suggests a large C sink capacity for the future in China, as forest biomass C accumulation generally increases with tree age and size [19,20]. Several recent studies have attempted to quantify the magnitude of future forest biomass C storage in China by using ground-based field measurements [21–24] and model simulations [25–27]. To simulate the trajectories of forest biomass changes with stand age, a general idea is to construct a relationship between forest biomass increment and forest age (as a proxy for forest development [18]). However, the previous studies do not generally consider the effects of forest demographic processes, such as age-related growth, or changes in environmental conditions (e.g., climate change and rising CO_2) in the age-biomass relationship [21,22].

It is widely acknowledged that environmental factors that increase forest growth, such as climate change and increasing atmospheric CO_2 concentration are primarily responsible for forest biomass C accumulation [28,29]. Climate change has been shown to significantly affect forest biomass C density [30,31], but its impact may differ among regions [32–36] and among forest types [25,37]. The effect of increasing CO_2 concentration on productivity

* Corresponding author.
E-mail address: slpiao@pku.edu.cn (S. Piao).

https://doi.org/10.1016/j.scib.2018.07.015
2095-9273/

has been widely documented in free-air CO_2 enrichment (FACE) experiments conducted in temperate forests (e.g., [38,39]), but these site-level results cannot simply be extrapolated to large areas because of the nonlinear physiological response to increasing CO_2 [38]. Additionally, real forest ecosystems experience a gradual increase in CO_2, rather than the sharp increase in CO_2 that is utilized in FACE experiments. Fortunately, the spatial and temporal effects of CO_2 fertilization on forest biomass can be determined from the analysis of earth system model (ESM) simulations, in which the CO_2 concentration is gradually increased at a prescribed rate. To simulate future forest biomass C sequestration realistically, it is essential to incorporate the effects of both climate change and steadily increasing CO_2 into the models.

Here, our main objective is to estimate both the separate and integrated effects of age-related forest regrowth, climate change and the rising CO_2 concentration on future forest biomass C accumulation in China by synthesizing *in situ* measurements and the results of model experiments. We use model experiments made under different socioeconomic scenarios, and also biogeochemical diagnostic experiments run for the fifth phase of the Coupled Model Intercomparison Project (CMIP5) [40]. We first established a statistical model of forest age-biomass C density which includes the effects of climatic factors. This model was then used to quantify the proportion of the forest biomass C sequestration capacity from the 2000s to the 2040s which can be attributed to forest age and climate change. The effect of rising CO_2 concentration on forest biomass C sequestration capacity was determined through analysis of the 1% a^{-1} CO_2 diagnostic experiments run in CMIP5.

2. Materials and methods

2.1. Field measurement data

Luo et al. [41] reviewed almost all forest biomass publications from 1978 to 2008, and collated forest biomass and associated site information. The resulting dataset included location, forest type, stand age, stand density, stand volume, mean tree height and diameter at breast height (DBH), as well as site-level aboveground and belowground forest biomass. Three filtering criteria were applied to ensure the representativeness, quality, authenticity and comparability of the data: (1) the collected data are confined to stably growing forest stands; (2) only biomass measurement data (oven-dried weight) based on a normative biomass survey can satisfy the data collection requirement; and (3) abnormal biomass data should pass professional judgment. There are 1011 records that include forest type, age, biomass, mean annual temperature (MAT) and mean annual precipitation (MAP) and satisfy the filtering criteria. The geographical distribution of these 1011 plots is shown in Fig. S1 (online). The full dataset was grouped into 14 forest types. The details of each forest type are listed in Table S1 (online). Biomass was converted into C content using a conversion factor of 0.5 [42].

2.2. Maps of forest distribution and forest age

According to the 1:1,000,000 Vegetation Map of China [43], the forest distribution data covers 161 plant biomes, which are further grouped into 14 categories based on the criterion adopted for field measurements described above. The 14 forest types are *Picea - Abies*, *Larix* spp., *Pinus tabuliformis*, other temperate *Pinaceae* spp., *Cunninghamia lanceolata*, *Pinus massoniana*, other warm *Pinaceae* spp., typical deciduous broadleaf forest (typical DBF), *Betula - Populus*, subtropical deciduous broadleaf forest (subtropical DBF), typical evergreen broadleaf forest (typical EBF), other subtropical evergreen broadleaf forest (other subtropical EBF), temperate mixed forest (temperate MF) and subtropical mixed forest (subtropical MF). The specific distribution areas and mean climatic conditions of these 14 forest categories are listed in Table S1 (online). The map of forest distribution was resampled to 1 km × 1 km resolution using the nearest neighbor approach.

A forest age map at a spatial resolution of 1 km × 1 km was generated by downscaling the provincial-level national forest inventory data using climate data and tree height data derived from light detection and ranging (LiDAR) data [16]. This dataset has been validated against the 8th forest inventory statistics (2009–2013) [16]. For example, in terms of area of each forest age class, the difference between downscaled stand age based on age-height relationships and stand age from forest inventory data is no more than 3% [16]. Moreover, there is a high coherence between downscaled stand age and forest inventory in most of forest types. Zhang et al. [44] (from Nanjing University) also released a Chinese national forest age map using the LiDAR-based forest height through establishing the relationship between forest age and tree height derived from field measurements. The mean forest age across China used in this study (~ 42.6 years) is comparable to that from Zhang et al. [44] (43 years in 2005). In addition, the five forest age classes have the similar fraction between the two national age datasets (young: 31.1% *vs* 38.2%, middle-aged: 34.8% *vs* 31.2%, premature: 16.3% *vs* 13.1%, mature: 10.7% *vs* 11.3%, overmature: 6.6% *vs* 6.2%) [16,44].

2.3. Historical climate data

We calculated MAT and MAP for the period 2001–2010 from the China Surface Meteorological Forcing Dataset. This dataset, which has a spatial resolution of 0.1° × 0.1° and a 3-hour temporal resolution, was generated by the hydro-meteorological research group at the Institute of Tibetan Plateau Research, Chinese Academy of Sciences, by merging observations from meteorological stations with model reanalysis [45,46]. Temperature data are obtained by merging China Meteorological Administration (CMA) observations with the Princeton meteorological forcing dataset [47]. Precipitation data are derived from the integration of Tropical Rainfall Measuring Mission data products [48], CMA operational observation stations, and Asian Precipitation–High Resolution Observational Data Integration Toward Evaluation of Water Resources data [49]. The 3-hourly climate datasets are aggregated into annual values, and then resampled to a 1 km × 1 km spatial resolution to match the maps of forest age and forest distribution.

2.4. Earth system model (ESM) simulations

Outputs from six ESMs participating in the fifth phase of the CMIP5 were analyzed (Table S2 online). The six EMSs used in this study are CanESM2, GFDL-ESM2M, HadGEM2-ES, IPSL-CM5A-LR, MPI-ESM-LR and NorESM1-ME. We used CO_2 concentration-forced historical simulations and future projections under three different Representative Concentration Pathways (RCP2.6, RCP4.5 and RCP8.5). The monthly temperature and precipitation were selected from the ESMs outputs. We also extracted monthly C mass in land vegetation (cVeg) from the 1% a^{-1} CO_2 experiments. The monthly values of temperature and cVeg for each year were averaged to give annual values and the precipitation values summed to give annual totals. All the ESM outputs were resampled to a 0.5° × 0.5° spatial resolution by using Climate Data Operators.

Since climate simulations from CMIP5 models are generally biased compared to observations, we applied corrections to the climate model temperature and precipitation simulation data based

on the MAT and MAP "observations" from the China Meteorological Forcing Dataset [45,46] for the period 2001–2010.

$$\widetilde{tas}_t^{\,sim} = tas_{t_0}^{obs} + (tas_t^{sim} - tas_{t_0}^{sim}), \quad (1)$$

$$\widetilde{pr}_t^{\,sim} = pr_{t_0}^{obs} + (pr_t^{sim} - pr_{t_0}^{sim}), \quad (2)$$

where $tas_{t_0}^{obs}$ and $pr_{t_0}^{obs}$ are the MAT and MAP during 2001–2010 based on the China Meteorological Forcing Dataset [45,46]. tas_t^{sim} and pr_t^{sim} are the MAT and MAP during period t from the ESM outputs. $\widetilde{tas}_t^{\,sim}$ and $\widetilde{pr}_t^{\,sim}$ are the corrected values of MAT and MAP during period t. These bias-corrected climate data were used to estimate forest biomass in the near future. The corrected climate data shows that, within the domain of our study, the annual temperature is predicted to increase by 1.1 °C (RCP2.6), 1.3 °C (RCP4.5) and 1.8 °C (RCP8.5) by the 2040s compared with the reference period of the 2000s (Fig. S2a online). Annual precipitation is predicted to increase slightly over the same period, albeit with large fluctuations (Fig. S2b online).

2.5. Analysis

Initially, we compiled a list of functions that have previously been applied in the modeling of forest growth (e.g. theoretical growth equations). These functions are listed in Table S3 (online). We then adapted these different model formulations of the relationship between forest age and biomass C density to include climate factors (MAT and MAP) as additional drivers of forest biomass C density. The adaptation consisted of adding a linear combination of MAT and MAP (i.e., $\alpha\times$MAT+$\beta\times$MAP+γ) into the model formulation as coefficient terms (Table S3 online). We then used the non-linear least square regression to find the optimized parameters for each function. R^2 and root mean square error (RMSE) were used as statistical criteria to determine which function form is most suitable for estimating the forest biomass density at the plot level. For each forest type, the function with the highest R^2 and the lowest RMSE is denoted in Table S1 (online) as "Fitted function".

We used forest biomass C storage and forest age data during the 2000s as references values. To quantify the effect of changing forest age on forest biomass C storage from the 2010s to 2040s, forest age varied inter-annually, whereas climate conditions are held constant at the average level of the 2000s. We defined this simulation scenario as CLIM-AGE.

$$B_{2000s}^{t} = f(age_t, MAT_{2000s}, MAP_{2000s})\; t = 2000s, 2010s, \ldots 2040s, \quad (3)$$

$$\triangle B_t^{age} = B_{2000s}^{t} - B_{2000s}^{2000s}, \quad (4)$$

where B denotes forest biomass C storage, and the superscript and subscript text in B denote the time periods corresponding to forest age and climate conditions, respectively. For instance, B_{2000s}^{t} represents forest biomass C storage calculated based on the forest age structure during time period t and the average climate conditions of the 2000s. f is a factor corresponding to one of the model formulations listed in Table S1 (online). age_t represents the forest age during time period t (t = 2000s, 2010s, … 2040s). MAT_{2000s} and MAP_{2000s} are the MAT and MAP during the 2000s, respectively. $\triangle B_t^{age}$ thus reflects the age-related biomass C increment during the specific time period t relative to the reference period of the 2000s.

We also calculate the uncertainty of forest biomass density based on the uncertainty in the forest age estimates. Uncertainties of forest age product are derived from the error map of the remotely-sensed forest height [16]. For each pixel, we consider 100 samples of normally distributed random forest age along with its mean value and variance (age uncertainty estimate). Correspondingly, we obtain 100 estimates of forest biomass density based on these randomly generated forest ages. The standard deviation of these 100 estimates is thus regarded as the uncertainty (or the error range) of forest biomass density.

To estimate climate change-induced changes in total forest biomass C storage, we allow both forest age and climate conditions to vary. This mode is denoted VARY-AGE.

$$B_t^t = f(age_t, MAT_t, MAP_t), \quad (5)$$

$$\triangle B_t^{clim} = B_t^t - B_{2000s}^t, \quad (6)$$

where B_t^t represents the biomass calculated based on the forest age structure during time period t and climate conditions in the same period. MAT_t and MAP_t are the MAT and MAP during period t, respectively. The effect of climate change on forest biomass C storage in time period t ($\triangle B_t^{clim}$) is obtained by subtracting the age-related biomass C increment (B_{2000s}^t, CLIM-AGE) from B_t^t (VARY-AGE).

To estimate the effect of increasing CO_2 concentration on forest biomass C storage, we used a CO_2 experiment (1% CO_2) in which a simulation of 140 years is performed using a 1% per year increase in CO_2 concentration. In this experiment, it is only the CO_2 concentration which changes with time. The other forcing parameters (like climate data inputs) are maintained at their pre-industrial values. For each pixel, we first determined the evolution of the CO_2 concentration and its corresponding vegetation C density from the 1% CO_2 experiment results. Linear interpolation was then applied to estimate the forest biomass C densities corresponding to the mean CO_2 concentration in 1978–2008, and in the 2010s–2040s, for each of the RCP scenarios. The effect of increasing CO_2 concentration on the forest biomass C density (F) was then expressed as the ratio of forest biomass C density at the mean CO_2 concentration during a specific period (e.g., the 2010s) under a certain RCP (e.g., RCP2.6) to that at the mean CO_2 concentration of 1978–2008.

$$F = \frac{C_t^{CO_2}}{C_{t_0}^{CO_2}}, \quad (7)$$

$$\triangle B_t^{CO_2} = (F-1) \times B_{2000s}^t, \quad (8)$$

where $C_t^{CO_2}$ denotes the biomass C density corresponding to the mean CO_2 concentration during period t from the 1% CO_2 experiment. t_0 denotes the period 1978–2008 (when field data were collected).

$$B_t^{full} = B_{2000s}^{2000s} + \triangle B_t^{age} + \triangle B_t^{clim} + \triangle B_t^{CO_2}. \quad (9)$$

Therefore, B_t^{full} represents the biomass C density in the time period t when age-related, climate change and CO_2 fertilization effects are all included.

3. Results

3.1. Evaluation of age-related statistical models for estimation of forest biomass C storage

Fig. 1 shows the values calculated by the optimal model formulation for each forest type. In general, these models could predict the forest biomass C density at the site level with acceptable values of R^2 and RMSE (Fig. 1). The best model performance was achieved in estimating the biomass C density of *Picea – Abies*, and second best for subtropical DBF. The explanatory power (in terms of R^2)

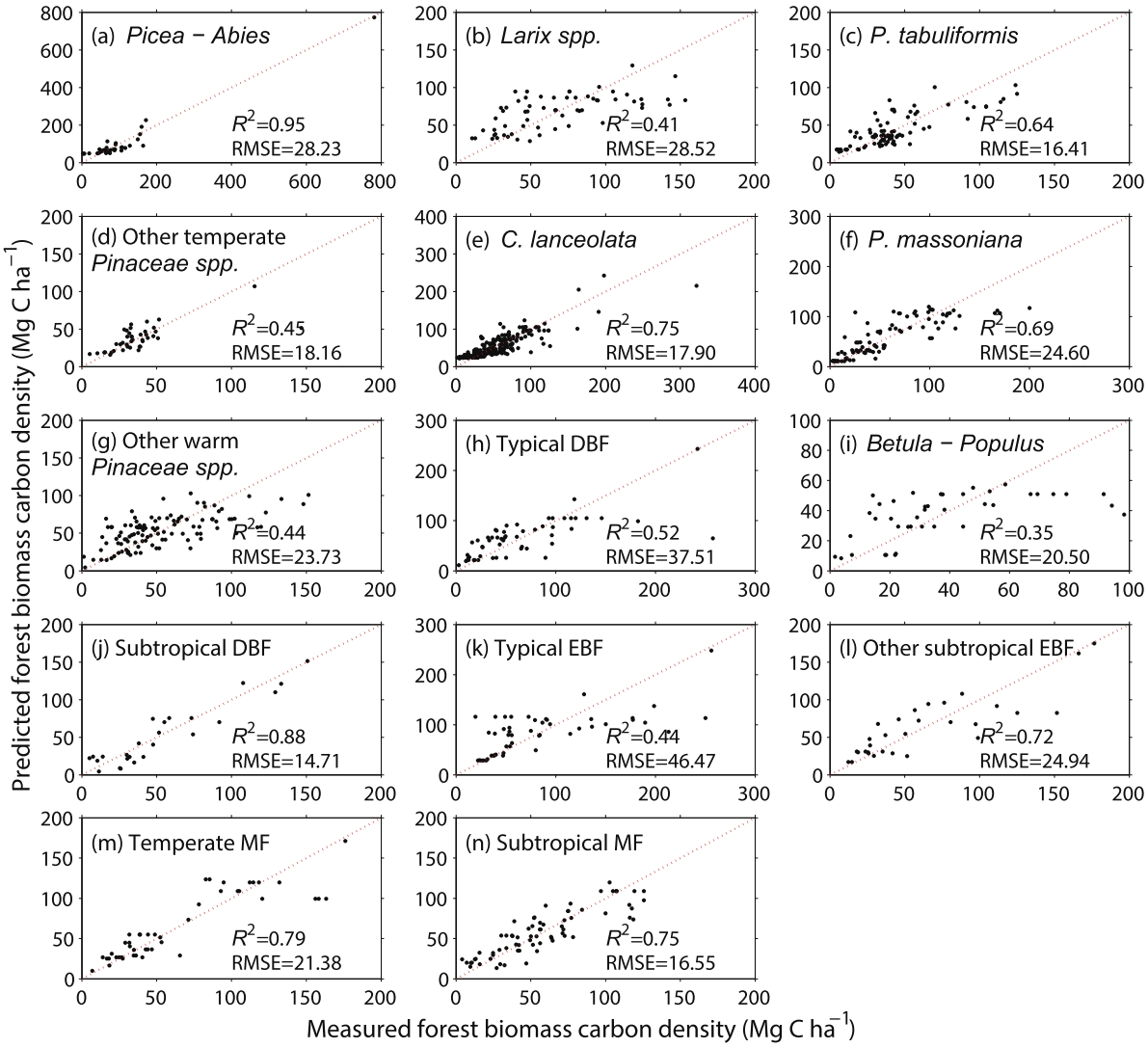

Fig. 1. Comparison between predicted forest biomass carbon density and measured values. The red dashed line in each subplot represents the 1:1 line. Performance of the nonlinear fitting function was gauged using the R^2 and root mean square error (RMSE) of each subplot for each forest type.

of the selected models exceeded 0.50 for nine forest types, and was greater than 0.70 for six forest types. The RMSE values of the selected models, across all 14 forest types ranged between 14.71 and 46.47 Mg C ha^{-1}. We also re-fit the biomass prediction model without the seemingly anomalous biomass observation data. For each forest type, we used three standard deviation above the mean as a threshold to filter out these seemingly anomalous biomass data. Among 14 forest types in our study, the filtered data are detected in 7 forest types As shown in Fig. S3 (online), the function fitting without these seemingly anomalous data would not significantly affect the plot-level biomass prediction except *Picea – Abies* (Fig. S3 online).

3.2. Age-related forest biomass C sequestration

Using the optimal model for each forest type, we mapped the spatial distribution of forest biomass C density during the 2000s. The total Chinese forest biomass C storage during the 2000s is estimated to be (10.75 ± 0.005) Pg C, with a mean forest biomass C density of 71.9 Mg C ha^{-1}. Typical DBF is the forest type which accounts for the largest fraction (27.5%) of total forest biomass C storage. The second largest fraction (18.5%) is due to *P. massoniana* (Fig. S4a online). Forest types with contributions larger than 10% of the total forest biomass C storage include typical EBF and *Picea – Abies*. In contrast, *P. tabuliformis*, temperate MF and subtropical MF all contribute very small amounts to the total forest biomass C storage, mainly due to their relatively small forest coverage areas. In terms of forest biomass C density, other subtropical EBF has the highest value (162.8 Mg C ha^{-1}), and typical DBF is second (94.5 Mg C ha^{-1}). There is high spatial heterogeneity in forest biomass C density. For instance, forest biomass C density is relatively low in northern China, central China and the southwestern area, with values generally below 40 Mg C ha^{-1} (Fig. S4b online). Forest biomass C density in Daxing'anling and parts of the southeastern area ranges from 60 to 80 Mg C ha^{-1} (Fig. S4b online). The Changbai Mountains and the southeastern Tibetan Plateau exhibit relatively high densities, which can exceed 100 Mg C ha^{-1} (Fig. S4b online).

When climate conditions are kept constant at the average level of the 2000s, and only the increase in forest age is considered (CLIM-AGE), the total forest biomass C storage increased from (10.75 ± 0.005) Pg C during the 2000s to (17.44 ± 0.005) Pg C in the 2040s. Interestingly, the decadal increase rate of forest biomass C storage decreased from 2.52 Pg C decade^{-1} in the 2010s to 1.09 Pg C decade^{-1} in the 2040s. In terms of the effect of forest age increment on forest biomass C storage in different forest types,

P. massoniana and typical DBF contribute more than 50% of the age-related increase in total forest biomass C storage. The annual rate of forest biomass C density increase due to forest age increment in *C. lanceolata* (3.49 Mg C ha^{-1} a^{-1}) and typical EBF (1.61 Mg C ha^{-1} a^{-1}) are the highest of all the forest types. In contrast, the lowest rate is found in *Larix* spp. forest (0.06 Mg C ha^{-1} a^{-1}). Further analysis of the spatial distribution indicates that the most obvious age-related forest biomass C accumulation appears in the southern Changbai Mountains, southeastern China and the southeastern Tibetan Plateau, with magnitudes exceeding 50 Mg C ha^{-1} during the period from the 2000s to the 2040s (Fig. S4b–f online). By the 2040s, the largest forest biomass C density is found in the southeastern Tibetan Plateau and southern Changbai Mountains, with regional values exceeding 140 Mg C ha^{-1}. Values in the southeastern area exceed 120 Mg C ha^{-1} (Fig. S4f online). By contrast, the increase in biomass C density is <40 Mg C ha^{-1} in northern China, central China and the southwestern area. There was no significant age-related forest C accumulation in the northern region of Daxing'anling during the 2000s to 2040s.

3.3. Effect of climate change on forest biomass C sequestration

Here, we forced the optimal model for each forest type with reconstructed climate data from the 2010s to the 2040s while varying forest age (hereafter referred to as VARY-AGE). Comparison of the CLIM-AGE results with those from VARY-AGE enables us to estimate the effect of climate change on changes in forest biomass C storage. We used climate simulations from six CMIP5 models to characterize the uncertainty of future climate change under each RCP scenario. During the 2010s, climate change induces an increase in forest biomass C storage of between (0.04 ± 0.17) and (0.11 ± 0.16) Pg C depending on the particular RCP scenario (Fig. 2). By the 2040s, the increase ranges from (0.52 ± 0.29) to (0.60 ± 0.20) Pg C. Although the mean response of forest biomass to climate change is positive under each RCP scenario, there is great uncertainty in the change of total forest biomass C storage (in terms of magnitude and even direction) estimated using different climate projections (Fig. S5 online). When comparing different time periods, the positive impact of climate change on forest biomass C storage is consistently observed among all three climate projections during the 2040s (Fig. S5 online). The effect of climate change differs among forest types (Fig. 3). For example, climate change is favorable in all scenarios for biomass C accumulation in *Picea - Abies*, *P. tabuliformis*, typical EBF, temperate MF and subtropical MF forests (Fig. 3). In contrast, a negative effect is observed in other temperate *Pinaceae* spp. and other subtropical EBF (Fig. 3). For *C. lanceolata*, the climate change impact is nearly neutral (Fig. 3).

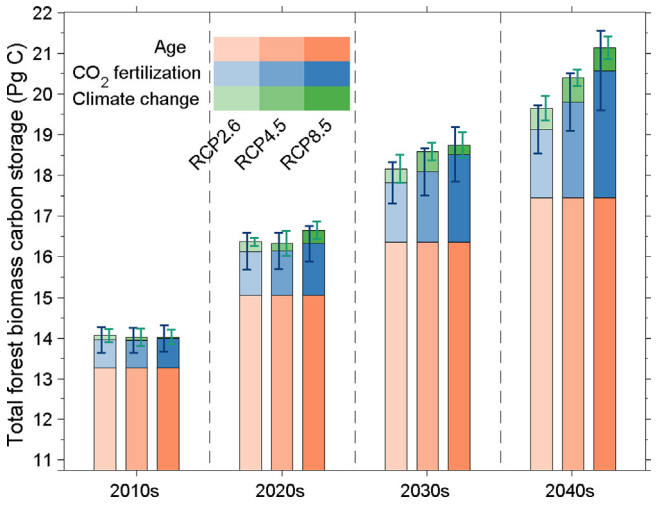

Fig. 2. Total forest biomass carbon storage during the 2010s to 2040s which is attributable to forest age, climate change and rising CO_2 under each Representative Concentration Pathway (RCP) scenario (RCP2.6, RCP4.5, and RCP8.5).

To quantify the contribution of only temperature (or only precipitation) change to changes in forest biomass C storage during the different time periods (2010s, 2020s, 2030s and 2040s), we forced the optimal model for each forest type by varying forest age, holding precipitation (or temperature) constant, and varying temperature (or precipitation). Our results show that the effect of precipitation change alone on biomass C storage is positive during the 2040s in each of the three scenarios, albeit with large uncertainties (Fig. S6 online). Precipitation changes contribute to an additional ~0.60 Pg C of forest biomass C accumulation by the 2040s (0.59 ± 0.30) Pg C under RCP2.6, (0.65 ± 0.22) Pg C under RCP4.5, (0.61 ± 0.31) Pg C under RCP8.5. The temperature effect is much smaller than the precipitation effect, and the overall warming impact on forest biomass C accumulation is negative during all periods studied in all three scenarios (Fig. S6 online). Although the effect of climate change on the change in total forest biomass C storage is driven mainly by changes in precipitation, the relative roles of temperature and precipitation changes in determining forest biomass C accumulation vary among forest types (Fig. S7 online). For example, warming is conducive to biomass C accumulation in *Picea – Abies*, *Betula – Populus*, typical EBF, and subtropical MF, but such warming is unfavorable for biomass C accumulation in other temperate *Pinaceae* spp., typical DBF, subtropical DBF, and other subtropical EBF (Figs. S7 and S8 online). Increased precipitation strongly stimulates biomass C accumulation in typical DBF and temperate MF during the 2030s and 2040s under all the three scenarios (Figs. S7 and S9 online).

3.4. Effect of increasing CO_2 concentration on forest biomass C sequestration

In the output of the 1% CO_2 experiments, vegetation C storage is found to increases monotonously with atmospheric CO_2 concentration. This fertilization effect of rising CO_2 concentration on forest biomass C storage can be represented as a ratio (see Methods). Increasing CO_2 concentration could increase forest biomass C sequestration by 1.68–3.12 Pg C across the three RCP scenarios by the 2040s compared to the scenario that only consider the forest age effect (Fig. 2). There is still great uncertainty in the CO_2 fertilization effect, however, as illustrated by the error bars in Fig. 2. For example, by the 2040s, the mean uncertainty of the CO_2 fertilization effect on forest biomass C sequestration may reach 0.76 Pg C (based on an average of the values of 0.59, 0.71 and 0.97 Pg C obtained for scenarios RCP2.6, RCP4.5 and RCP8.5, respectively), which is greater than the magnitudes of the climate change effect on the biomass increase. The fertilization effect may also vary with forest type. Fig. 3 shows that particularly large CO_2 fertilization effects were found in *C. lanceolata* (20.3 Mg C ha^{-1} under RCP2.6; 28.9 Mg C ha^{-1} under RCP4.5; 37.5 Mg C ha^{-1} under RCP8.5) and other subtropical EBF (14.2 Mg C ha^{-1} under RCP2.6; 20.5 Mg C ha^{-1} under RCP4.5; 29.2 Mg C ha^{-1} under RCP8.5) by the 2040s compared to the projections which only include the effects of forest age (Fig. 3).

3.5. Chinese forests biomass C sequestration potential in the future

Biomass C storage in Chinese forests could reach (19.64 ± 0.58) Pg C (RCP2.6), (20.38 ± 0.78) Pg C (RCP4.5), and (21.12 ± 1.06) Pg C (RCP8.5) by the 2040s if the effects of forest age, climate change and rising CO_2 levels are integrated (Fig. 2). Under each scenario,

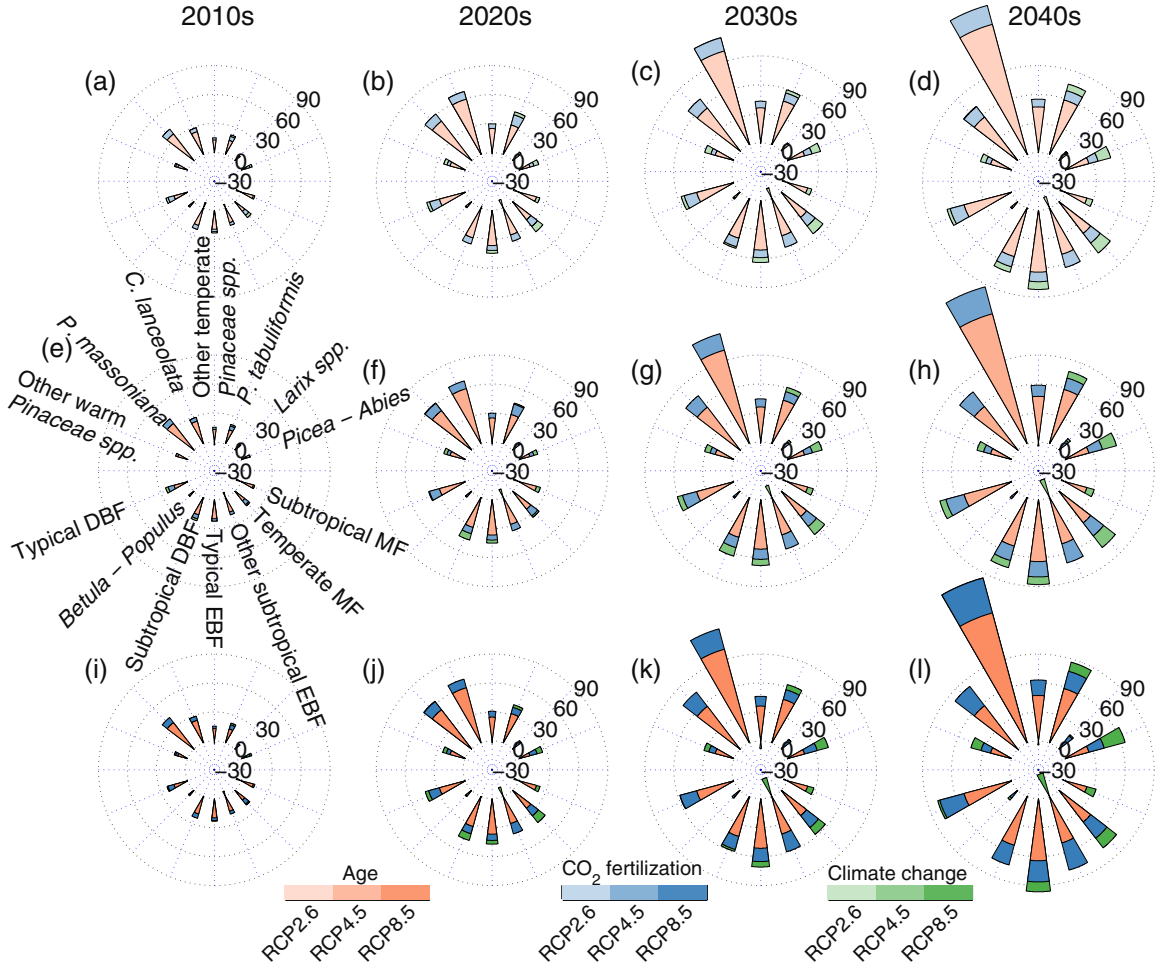

Fig. 3. The effects of forest age, climate change and increasing CO_2 concentration on biomass carbon density in each forest type under the RCP2.6 (a–d), RCP4.5 (e–h) and RCP8.5 (i–l) scenarios compared to the reference period (2000s). The panels in the four columns indicate the periods of the 2010s, 2020s, 2030s and 2040s. Units: Mg C ha^{-1}.

the increase in forest biomass C sequestration due to forest age outweighs that due to the CO_2 fertilization effect. The climate change effect, while positive, is much smaller than either the effect of forest age increment or rising CO_2 concentration. For example, under RCP8.5, the CO_2 fertilization effect on forest biomass C sequestration is only half that of the stimulating effect of forest age increase, and climate change-induced increase in C sequestration is only one-tenth of that due to forest age increase. It is notable that the total forest biomass C sequestration rate from the 2000s to 2040s is estimated to be ~0.26 Pg C a^{-1} under RCP8.5, a rate which could offset ~10% of contemporary greenhouse gas CO_2 emissions (~2.70 Pg C during the 2010s).

4. Discussion and conclusion

To map forest biomass C storage, we developed an optimal semi-empirical model using forest biomass C density, forest age and climatic factors for each forest type, based on the plot data for each forest type. In contrast to previous studies, we used climatic variables (MAT and MAP) to establish forest age-biomass relationships. These semi-empirical models can predict biomass C density at the plot level with acceptable skill, suggesting that our choice of candidate models is reasonable. Using the highest R^2 and the lowest RMSE as statistical criteria to select the optimal model for each forest type ensures the best possible fit to the field observations is achieved. Based on the optimal model established for each forest type, total forest biomass C storage in China was estimated to be (10.75 ± 0.005) Pg C during the 2000s. Most previous attempts to determine total forest biomass C storage in China have used national forest inventory data [14,50–53], and have produced values lower than our estimate. For example, Zhang et al. [14] used repeated national forest inventories that provided information on the stock volume and area of the dominant tree species in several age groups over different administrative units to estimate forest biomass C storage. Their approach produced an estimate of ~6.24 Pg C. The discrepancies in the estimate obtained using the different methods vary with forest type. If we consider the mean biomass C densities derived for different forest types and compare them with values obtained from the 7th inventory [54], we find the values for *Picea – Abies* (77 Mg C ha^{-1} *vs* 81 Mg C ha^{-1}), *P. tabuliformis* (33 Mg C ha^{-1} *vs* 29 Mg C ha^{-1}), and *Betula – Populus* (33 Mg C ha^{-1} *vs* 39 Mg C ha^{-1}) are in relatively good agreement. In contrast, our estimates are approximately double the values obtained from inventory data for *Larix* spp. (70 Mg C ha^{-1} *vs* 33 Mg C ha^{-1}), *P. massoniana* (62 Mg C ha^{-1} *vs* 27 Mg C ha^{-1}), and typical DBF (94 Mg C ha^{-1} *vs* 45 Mg C ha^{-1}). Some of the difference between the values obtained using different methods may be attributable to the fact that field measurements of forest biomass are generally higher than those reported at the province level in Chinese forest inventory data [14,55]. Difference between stand age distribution data obtained from field measurements and those derived from the LiDAR-based forest age map could also lead to differences in forest biomass C storage estimates. Fig. S10 (online) shows that there is an

extremely significant difference ($P < 0.01$, Kolmogorov-Smirnov test) between the frequency distribution of stand age obtained from field measurements and that obtained from the forest age map. For the field measurements, young forest is dominant, with middle-age and mature stage forests undersampled in comparison to the national forest age distribution. Since forests in the early growth stages have a faster C accumulation rate than those in later stages, the extrapolation of field observation made in young forest to middle-aged and mature stage forests could lead to an overestimation of biomass.

Support for our relatively high estimate of total forest biomass C storage in China comes from a growing number of studies that integrate field measurements with spatial satellite observations (e.g., tree height, vegetation indices, land cover) to map forest biomass C density [51,52,56–59]. For example, using spaceborne LiDAR and forest inventory data, Su et al. [59] estimated that the mean aboveground biomass C density is ~60 Mg C ha^{-1} throughout China, which equates to a total forest biomass C density of ~74.4 Mg C ha^{-1} if the conversion ratio of total to aboveground biomass C density is assumed to have a value of 1.24 [60]. Yin et al. [61] integrated plot-level field measurements with satellite reflectance data and a vegetation index, to show that the aboveground forest biomass C density was 56.1 Mg C ha^{-1} during the 2000s, which equates to a total forest biomass C density of 69.6 Mg C ha^{-1} using the same conversion ratio. These results are similar to our estimate of forest biomass C density of 71.9 Mg C ha^{-1} during the 2000s.

In agreement with previous studies [50,51], we found that the southeastern Tibetan Plateau has the greatest biomass C density, whereas southeast China has a relatively low density. This distribution occurs because the southeastern Tibetan Plateau has favorable climatic conditions, a relatively cool temperature and moderately high precipitation that can support fast forest growth and slow decomposition [62], while the forests in southeast China are generally characterized by a young age structure [16]. Our finding that forest biomass C density in both the Changbai Mountains and Xiaoxing'anling in the northeastern region is greater than the value in Daxing'anling is also consistent with previous studies (e.g., [57,63]).

Stand age is a strong determinant of forest biomass C sequestration rates [19,64–68], and thus also forest biomass C storage [14]. Information on the forest's stage of development should therefore be included in predictions of the future trajectories of forest biomass C storage. Here, we showed that forest age change alone could increase biomass C stock by 6.69 Pg C from the 2000s to the 2040s (~0.17 Pg C a^{-1}). Our estimate is in agreement with the work of Xu [69], which showed that the forest age-related increase in biomass C storage from 2010 to 2050 will be ~6.5 Pg C (~ 0.16 Pg C a^{-1}) based on the logarithmic relationship between forest age and biomass. However, our result is larger than that of Hu et al. [22], who constructed an age-based matrix model using continuous forest inventory datasets and found that the overall increase in forest biomass C storage will be ~3.55 Pg C from 2005 to 2050 (~ 0.079 Pg C a^{-1}). We also found that the amount of decadal forest biomass C sequestration capacity during the 2010s (2.52 Pg C) will decrease by more than 50% during the 2040s (1.09 Pg C). This decline in forest biomass C sequestration with increasing stand age can be partially attributed to declining net primary productivity (NPP) [70–73], although forest C sequestration generally increases with tree age and size at the stand level [20]. Prior studies conducted at the regional scale also reported age-related increases in forest biomass C density, albeit of different magnitudes. For example, Sun et al. [74] found that forest biomass C density on the southeastern Tibetan Plateau increased by ~16 Mg C ha^{-1} from 2001 to 2050 (>50 Mg C ha^{-1} in our study), based on the forest age-biomass C density relationship found in 413 field measurements. Since Sun et al. [74] used a similar forest stand age map to that used in this study, the difference between our study and Sun et al. [74] is attributed to the number of samples (413 versus 1011 samples in our study) and the use of fitting functions to construct the forest age-biomass C density relationship (logistic curve versus the species-specific fitting equations applied in our study). In addition, stand age-driven changes in forest biomass C storage also differ among forest types because of their species-specific physiological growth traits. Fast-growing needle-leaf forests, such as *C. lanceolata* and *P. massoniana*, display relatively large forest biomass C sequestration rates. Zhao et al. [75] found that *C. lanceolata* has larger NPP than other Chinese forests using the 3-PG (Physiological Principles in Predicting Growth) model. In contrast, a relatively low growth rate was found in *Picea* - *Abies* forests (e.g., [76]). Our results highlight the fact that demographic factors play an important role in long-term forest biomass C sequestration capacity. The stand age effect should be considered in any process-based model of forest ecosystem C stocks and fluxes. For example, models could include the NPP-age relationship when simulating forest C stock during stand development (e.g., [77–79]).

In this study, we showed that ongoing climate change could exert positive impacts on forest biomass C sequestration capacity, but this effect is much smaller than the effect of increasing stand age. Furthermore, the positive effect of climate change is caused mainly by precipitation changes rather than by warming. Biomass C density in temperate forests is determined primarily by water availability [37], and we observed that it is significantly enhanced by increased precipitation. The sign of the warming effect on forest biomass C density depends on the background climate, and a positive effect can shift to a negative one if the background temperature exceeds a certain threshold value [30]. This finding tentatively suggests that the non-significant warming effect observed in this study could be due to regional compensation between contrasting temperature effects. However, a consensus on the effect of climate change on forest biomass C accumulation has still not been attained [80–83]. For example, Ju et al. [81] found that increasing temperature and precipitation may have a negative impact on forest productivity in most regions, except the western parts of southwest China and the northern part of southeast China. By contrast, Ni [82] noted that climate change alone would produce an increase in vegetation C storage, especially in mixed and evergreen broadleaf forests. We also showed that the effect of climate change differs among forest types [25], stand ages [33] and regions [36]. For example, ecosystems in the northern and western parts of China are more sensitive to climate change than those in the eastern region [84]. Climate change has been shown to increase forest stand mortality in some regions, undermining the vegetation growth effect [85]. Our results further highlight the fact that the observed non-uniform effects of climate change should not be overlooked when simulating the future trajectories of forest biomass C stock.

The future forest biomass C storage calculations presented here were based on uncorrected ESM climate data (Fig. S11 online). The MAP derived from uncorrected ESM data is 200 mm greater than the values derived from the corrected data. In contrast, the value of MAT obtained from the uncorrected ESM data is ~0.2 °C lower than the value obtained from the corrected data. Fig. S11 (online) shows that estimates of forest biomass C storage made using uncorrected ESM climate data are much higher than those based on the corrected climate data. The difference can be larger than 2 Pg C for all time periods under each scenario. Moreover, the uncertainty in the forest biomass prediction is also larger when the uncorrected data are used. Our analysis suggests that the forest C sequestration capacity based on uncorrected ESMs climate data would be an overestimate, and highlights the fact that ESM outputs need to be calibrated against observations to ensure that the most realistic projections of forest biomass C sequestration are obtained.

As is common practice, we use the "space-for-time substitution" framework to establish the relationship between forest bio-

mass density, age and climatic factors within each forest type. This technique is widely used in the projection of ecosystem responses to future climate change because of insufficient temporal data [86–88]. However, this approach could lead to bias in the results, since it assumes that the spatial and temporal variability in forest biomass density in response to climate change are equivalent [89,90]. Long-term field measurements are required if this potential issue for the accurate forecasting of future trajectories of forest biomass under changing climate regimes is to be overcomed.

The uneven distribution of sampling sites is another potential source of errors. In northwest China and Xinjiang, there are a rather limited number of samples for the dominant forest types, *Larix* spp. (2), *Betula-Populus* (5) and typical DBF (7). This lack of samples is partly due to the fact that the forest coverage in these regions is also scant. To avoid this limitation, we established the relationship between forest biomass density, age and climatic factors based on forest type rather than region. For all forest types, the number of sample sites is in the range 25 to 268. For the three dominant tree species in these regions, the R^2 of the constructed statistical model could reach 0.41 ($P < 0.01$), 0.35 ($P < 0.01$), 0.52 ($P < 0.01$), respectively, suggesting that these models have some statistical power in modeling forest biomass distribution. Even though the forest coverage is limited, and forest structures are relatively simple in northwestern China and Xinjiang, there may still be considerable spatial variability in forest biomass distribution. Ideally, more field samples are needed to further reduce the uncertainty.

In a significant advance over prior studies, we estimated the effect of rising CO_2 concentration on forest biomass in terms of the forest age-climate-biomass relationship. The responses of different forest types to climate change differed across our study area, whereas the effects of rising CO_2 concentration were much more consistent across forest biomes. Process-based model simulations show that China's role as a C sink over the past two decades was mainly due to the CO_2 fertilization effect, and that climate change alone would cause this area to become a C source [35]. We show that the magnitude of the CO_2 fertilization effect is comparable to the beneficial effect of increased stand age in some forest types, such as *Picea - Abies*. In addition, the CO_2 fertilization effect is larger than the negative warming impact on forest biomass C sequestration. However, we note that current ESMs do not include the effect of nutrient availability on vegetation growth, and thus the CO_2 fertilization effect might be overestimated [91]; this issue highlights the need for future assessments of forest biomass C sequestration capacity to consider the limitations imposed by soil fertility.

In this study, we quantified Chinese forest biomass C sequestration capacity in the near future, integrating the effects of stand development, climate change and increasing CO_2 concentration. While the link between forest biomass C density and forest age appears to be clear, few model formulations consider the interacting effects of climate change and forest age on forest biomass C sequestration capacity. We compared the performance of different empirical statistical functions in estimating plot-level biomass C density, and selected the optimal function form and/or parameters to predict the forest biomass C storage change in the future. In contrast, previous studies such as Xu et al. [24], He et al. [21] and Chen et al. [92] used only a logistics function to estimate biomass for different forest types. Moreover, we estimate the individual contribution of forest aging and climate change to the overall increase in forest biomass C storage. The individual effect of temperature and precipitation changes on forest biomass C storage are also separated out, by the method of keeping one climatic factor constant and allowing the other to vary. Our study therefore provide an analysis of climate change impacts on changes in forest biomass C storage, which has not been included in previous studies e.g. Xu et al. [24], He et al. [21] and Hu et al. [22]. Our results suggest that the forest age-induced increase in total forest biomass C sequestration has the greatest effect, highlighting the importance of previous afforestation programs in enhancing future forest C uptake [93]. The overall positive effect of climate change on forest biomass C sequestration is relatively small. Furthermore, increasing CO_2 concentration, which has always been omitted from prior studies, will also significantly contribute to future C sequestration. The response of different forest types to climate change and CO_2 fertilization and their growth characteristics should be taken into account when choosing species for future forest plantation.

Several caveats remain that should be examined in future studies. First, we used a fixed forest distribution map and did not consider changes in forest area. The Chinese government will likely continue to launch tree planting projects that further increase forest biomass C sequestration capacity [94], although such increase could be partially offset by the C loss due to potential wood harvesting and natural disturbances. Natural disturbances regimes like forest fires, insect outbreaks, and extreme weather events could cause tree mortality, defoliation and other growth inhibitions, which could further undermine the desired effects from forest regrowth and environmental change [95]. For example, Lü et al. [96] found that mean annual C emission due to forest fires in China is about 11.31 Tg C a^{-1}. The 1987 conflagration in northeastern China emitted 25–49 Tg C to the atmosphere [97]. Hence, our prediction of forest biomass C sequestration capacity might be an underestimate, if the aging effects from larger forest area outweighs the effect of disturbances. Second, the effect of nitrogen deposition on forest biomass C sequestration is ignored in this study. The trajectories of future biomass C sequestration would be more realistic if the effect of nitrogen deposition on forest biomass C sequestration could be incorporated into forest biomass predictive models. But the magnitude and direction of the contribution of nitrogen deposition to forest biomass C accumulation remain elusive [98–102]. A synthesis of experimental studies is required to elucidate the effect of nitrogen addition on forest biomass C sequestration capacity. Third, in accordance with prior studies (e.g., [19,103]), our results indicated that forest biomass C sequestration capacity over a decadal time scale has a much greater reliance on the disturbance regime than on climate change or increasing CO_2 concentration. This result suggests that current process-based models of forest growth and C dynamics, which assume that ecosystem dynamics are under equilibrium conditions, would not properly simulate forest regrowth processes [18] and could therefore underestimate biomass C accumulation in certain forest types [62]. This finding further highlights the importance of explicit representation of forest age dynamics following disturbance, which should be embedded within the current framework of process-based C cycle models (e.g., [104]).

Conflict of interest

The authors declare that they have no conflict of interest.

Acknowledgments

This work was supported by the National Key R&D Program of China (2017YFA0604702) and the National Natural Science Foundation of China (41530528 and 31621091).

Appendix A. Supplementary material

Supplementary data associated with this article can be found, in the online version, at https://doi.org/10.1016/j.scib.2018.07.015.

References

[1] Pan Y, Birdsey RA, Fang J, et al. A large and persistent carbon sink in the World's forests. Science 2011;333:988–93.
[2] Piao S, Fang J, Ciais P, et al. The carbon balance of terrestrial ecosystems in China. Nature 2009;458:1009–13.
[3] Schimel DS, House JI, Hibbard KA, et al. Recent patterns and mechanisms of carbon exchange by terrestrial ecosystems. Nature 2001;414:169–72.
[4] Bonan GB. Forests and climate change: forcings, feedbacks, and the climate benefits of forests. Science 2008;320:1444–9.
[5] Canadell JG, Raupach MR. Managing forests for climate change mitigation. Science 2008;320:1456–7.
[6] Canadell JG, Schulze ED. Global potential of biospheric carbon management for climate mitigation. Nat Commun 2014;5:5282.
[7] Dixon RK, Solomon AM, Brown S, et al. Carbon pools and flux of global forest ecosystems. Science 1994;265:185–90.
[8] Mackey B, Prentice IC, Steffen W, et al. Untangling the confusion around land carbon science and climate change mitigation policy. Nat Clim Change 2013;3:552–7.
[9] Gower ST. Patterns and mechanisms of the forest carbon cycle. Annu Rev Environ Resour 2003;28:169–204.
[10] Houghton R, Hall F, Goetz SJ. Importance of biomass in the global carbon cycle. J Geophys Res Biogeosci 2009;114:G00E03.
[11] Zhou W, Lewis BJ, Wu S, et al. Biomass carbon storage and its sequestration potential of afforestation under natural forest protection program in China. Chin Geog Sci 2014;24:406–13.
[12] State Forestry Administration of China. Forest Resource Statistics of China (2009–2013). Beijing; 2014.
[13] FAO. Global forest resources assessment 2010. Rome: UNFAO; 2010.
[14] Zhang C, Ju W, Chen JM, et al. China's forest biomass carbon sink based on seven inventories from 1973 to 2008. Clim Change 2013;118:933–48.
[15] Xu X, Cao M, Li K. Temporal-spatial dynamics of carbon storage of forest vegetation in China. Prog Geogr 2007;26:1–10 (in Chinese).
[16] Zhang Y, Yao Y, Wang X, et al. Mapping spatial distribution of forest age in China. Earth Space Sci 2017;4:108–16.
[17] Nelson R, Margolis H, Montesano P, et al. Lidar-based estimates of aboveground biomass in the continental US and Mexico using ground, airborne, and satellite observations. Remote Sens Environ 2017;188:127–40.
[18] Pan Y, Chen JM, Birdsey R, et al. Age structure and disturbance legacy of North American forests. Biogeosci 2011;8:715–32.
[19] Pregitzer KS, Euskirchen ES. Carbon cycling and storage in world forests: biome patterns related to forest age. Glob Change Biol 2004;10:2052–77.
[20] Stephenson NL, Das AJ, Condit R, et al. Rate of tree carbon accumulation increases continuously with tree size. Nature 2014;507:90–3.
[21] He N, Wen D, Zhu J, et al. Vegetation carbon sequestration in Chinese forests from 2010 to 2050. Glob Change Biol 2017;23:1575–84.
[22] Hu H, Wang S, Guo Z, et al. The stage-classified matrix models project a significant increase in biomass carbon stocks in China's forests between 2005 and 2050. Sci Rep 2015;5:11203.
[23] Huang L, Liu J, Shao Q, et al. Carbon sequestration by forestation across China: past, present, and future. Renew Sustain Energy Rev 2012;16:1291–9.
[24] Xu B, Guo Z, Piao S, et al. Biomass carbon stocks in China's forests between 2000 and 2050: a prediction based on forest biomass-age relationships. Sci China Life Sci 2010;53:776–83.
[25] Dai E, Wu Z, Ge Q, et al. Predicting the responses of forest distribution and aboveground biomass to climate change under RCP scenarios in southern China. Glob Change Biol 2016;22:3642–61.
[26] Zhang XQ, Xu DY. Potential carbon sequestration in China's forests. Environ Sci Policy 2003;6:421–32.
[27] Zhou L, Wang S, Kindermann G, et al. Carbon dynamics in woody biomass of forest ecosystem in China with forest management practices under future climate change and rising CO_2 concentration. Chin Geogr Sci 2013;23:519–36.
[28] Piao SL, Sitch S, Ciais P, et al. Evaluation of terrestrial carbon cycle models for their response to climate variability and to CO_2 trends. Global Change Biol 2013;19:2117–32.
[29] Piao SL, Liu Z, Wang YL, et al. On the causes of trends in the seasonal amplitude of atmospheric CO_2. Glob Change Biol 2018;24:608–16.
[30] Liu Y, Yu G, Wang Q, et al. How temperature, precipitation and stand age control the biomass carbon density of global mature forests. Glob Ecol Biogeogr 2014;23:323–33.
[31] McMahon SM, Parker GG, Miller DR. Evidence for a recent increase in forest growth. Proc Natl Acad Sci USA 2010;107:3611–5.
[32] Bennett AC, McDowell NG, Allen CD, et al. Larger trees suffer most during drought in forests worldwide. Nat Plants 2015;1:15139.
[33] Chen HYH, Luo Y, Reich PB, et al. Climate change-associated trends in net biomass change are age dependent in western boreal forests of Canada. Ecol Lett 2016;19:1150–8.
[34] Luo Y, Chen HYH. Observations from old forests underestimate climate change effects on tree mortality. Nat Commun 2013;4:1655.
[35] Piao S, Ito A, Li S, et al. The carbon budget of terrestrial ecosystems in East Asia over the last two decades. Biogeosci 2012;9:3571–86.
[36] Peng SS, Piao SL, Ciais P, et al. Asymmetric effects of daytime and night-time warming on Northern Hemisphere vegetation. Nature 2013;501:88–92.
[37] Piao SL, Yin GD, Tan JG, et al. Detection and attribution of vegetation greening trend in China over the last 30 years. Glob Change Biol 2015;21:1601–9.
[38] Hickler T, Smith B, Prentice IC, et al. CO_2 fertilization in temperate FACE experiments not representative of boreal and tropical forests. Glob Change Biol 2008;14:1531–42.
[39] Norby RJ, Warren JM, Iversen CM, et al. CO_2 enhancement of forest productivity constrained by limited nitrogen availability. Proc Natl Acad Sci USA 2010;107:19368–73.
[40] Taylor KE, Stouffer RJ, Meehl GA. An overview of CMIP5 and the experiment design. Bull Am Meteorol Soc 2012;93:485–98.
[41] Luo Y, Zhang X, Wang X, et al. Biomass and its allocation of Chinese forest ecosystems. Ecology 2014;95. 2026.
[42] Myneni RB, Dong J, Tucker CJ, et al. A large carbon sink in the woody biomass of Northern forests. Proc Natl Acad Sci USA 2001;98:14784–9.
[43] Editorial Board of Vegetation Map of China. Chinese Academy of Sciences. Vegetation Map of the People's Republic of China (1:1000000) (Digital version). Geology Press, Beijing; 2007.
[44] Zhang C, Ju W, Chen JM, et al. Mapping forest stand age in China using remotely sensed forest height and observation data. J Geophys Res Biogeosci 2014;119:1163–79.
[45] Chen Y, Yang K, He J, et al. Improving land surface temperature modeling for dry land of China. J Geophys Res Atmos 2011;116:D20104.
[46] Yang K, He J, Tang W, et al. On downward shortwave and longwave radiations over high altitude regions: observation and modeling in the Tibetan Plateau. Agric For Meteorol 2010;150:38–46.
[47] Sheffield J, Goteti G, Wood EF. Development of a 50-year high-resolution global dataset of meteorological forcings for land surface modeling. J Clim 2006;19:3088–111.
[48] Huffman GJ, Bolvin DT, Nelkin EJ, et al. The TRMM multisatellite precipitation analysis (TMPA): quasi-global, multiyear, combined-sensor precipitation estimates at fine scales. J Hydrometeorol 2007;8:38–55.
[49] Yatagai A, Arakawa O, Kamiguchi K, et al. A 44-year daily gridded precipitation dataset for Asia based on a dense network of rain gauges. Sola 2009;5:137–40.
[50] Chi H, Sun G, Huang J, et al. National forest aboveground biomass mapping from ICESat/GLAS data and MODIS imagery in China. Remote Sens 2015;7:5534–64.
[51] Du L, Zhou T, Zou Z, et al. Mapping forest biomass using remote sensing and national forest inventory in China. Forests 2014;5:1267–83.
[52] Sun Z, Peng S, Li X, et al. Changes in forest biomass over China during the 2000s and implications for management. For Ecol Manage 2015;357:76–83.
[53] Hu H, Yang Y, Fang J. Toward accurate accounting of ecosystem carbon stock in China's forests. Sci Bull 2016;61:1888–9.
[54] Li H, Lei Y, Zeng W. Forest carbon storage in China estimated using forestry inventory data. Sci Silvae Sin 2011;47:7–12.
[55] Guo Z, Fang J, Pan Y, et al. Inventory-based estimates of forest biomass carbon stocks in China: a comparison of three methods. For Ecol Manage 2010;259:1225–31.
[56] Baccini A, Goetz SJ, Walker WS, et al. Estimated carbon dioxide emissions from tropical deforestation improved by carbon-density maps. Nat Clim Change 2012;2:182–5.
[57] Piao SL, Fang JY, Zhu B, et al. Forest biomass carbon stocks in China over the past two decades: estimation based on integrated inventory and satellite data. J Geophy Res Biogeosci 2005;110:G01006.
[58] Saatchi SS, Harris NL, Brown S, et al. Benchmark map of forest carbon stocks in tropical regions across three continents. Proc Natl Acad Sci USA 2011;108:9899–904.
[59] Su Y, Guo Q, Xue B, et al. Spatial distribution of forest aboveground biomass in China: estimation through combination of spaceborne lidar, optical imagery, and forest inventory data. Remote Sens Environ 2016;173:187–99.
[60] Liu YY, van Dijk AIJM, de Jeu RAM, et al. Recent reversal in loss of global terrestrial biomass. Nat Clim Change 2015;5:470–4.
[61] Yin G, Zhang Y, Sun Y, et al. MODIS based estimation of forest aboveground biomass in China. PLoS One 2015;10. e0130143.
[62] Keith H, Mackey BG, Lindenmayer DB. Re-evaluation of forest biomass carbon stocks and lessons from the world's most carbon-dense forests. Proc Natl Acad Sci USA 2009;106:11635–40.
[63] Thurner M, Beer C, Santoro M, et al. Carbon stock and density of northern boreal and temperate forests. Glob Ecol Biogeogr 2014;23:297–310.
[64] Caspersen JP, Pacala SW, Jenkins JC, et al. Contributions of land-use history to carbon accumulation in US forests. Science 2000;290:1148–51.
[65] Song CH, Woodcock CE. A regional forest ecosystem carbon budget model: impacts of forest age structure and landuse history. Ecol Modell 2003;164:33–47.
[66] Vilen T, Gunia K, Verkerk PJ, et al. Reconstructed forest age structure in Europe 1950–2010. For Ecol Manage 2012;286:203–18.
[67] Liu S, Zhou T, Wei L, et al. The spatial distribution of forest carbon sinks and sources in China. Chin Sci Bull 2012;57:1699–707.
[68] Zhou L, Wang S, Zhou T, et al. Carbon dynamics of China's forests during 1901–2010: the importance of forest age. Sci Bull 2016;61:2064–73.
[69] Xu B. Research on the Relationship between Biomass and Age of Main Forest-types in China. Bachelor thesis. Beijing: Peking University, 2008 [in Chinese].
[70] Goulden ML, McMillan AMS, Winston GC, et al. Patterns of NPP, GPP, respiration, and NEP during boreal forest succession. Glob Change Biol 2011;17:855–71.

[71] Ryan MG, Binkley D, Fownes JH. Age-related decline in forest productivity: pattern and process. Adv Ecol Res 1997;27:213–62.
[72] Ryan MG, Binkley D, Fownes JH, et al. An experimental test of the causes of forest growth decline with stand age. Ecol Monogr 2004;74:393–414.
[73] Wang CK, Bond-Lamberty B, Gower ST. Carbon distribution of a well- and poorly-drained black spruce fire chronosequence. Glob Change Biol 2003;9:1066–79.
[74] Sun X, Wang G, Huang M, et al. Forest biomass carbon stocks and variation in Tibet's carbon-dense forests from 2001 to 2050. Sci Rep 2016;6:34687.
[75] Zhao M, Xiang W, Peng C, et al. Simulating age-related changes in carbon storage and allocation in a Chinese fir plantation growing in southern China using the 3-PG model. For Ecol Manage 2009;257:1520–31.
[76] Ni J, Zhang XS, Scurlock JMO. Synthesis and analysis of biomass and net primary productivity in Chinese forests. Ann For Sci 2001;58:351–84.
[77] Wang S, Chen JM, Ju WM, et al. Carbon sinks and sources in China's forests during 1901–2001. J Environ Manage 2007;85:524–37.
[78] Wang S, Zhou L, Chen J, et al. Relationships between net primary productivity and stand age for several forest types and their influence on China's carbon balance. J Environ Manage 2011;92:1651–62.
[79] Williams CA, Collatz GJ, Masek J, et al. Carbon consequences of forest disturbance and recovery across the conterminous United States. Glob Biogeochem Cycles 2012;26:GB1005.
[80] Cao MK, Prince SD, Li KR, et al. Response of terrestrial carbon uptake to climate interannual variability in China. Glob Change Biol 2003;9:536–46.
[81] Ju WM, Chen JM, Harvey D, et al. Future carbon balance of China's forests under climate change and increasing CO_2. J Environ Manage 2007;85:538–62.
[82] Ni J. Carbon storage in terrestrial ecosystems of China: estimates at different spatial resolutions and their responses to climate change. Clim Change 2001;49:339–58.
[83] Zhao M, Zhou GS. Carbon storage of forest vegetation in China and its relationship with climatic factors. Clim Change 2006;74:175–89.
[84] Ni J. Impacts of climate change on Chinese ecosystems: key vulnerable regions and potential thresholds. Reg Environ Change 2011;11:S49–64.
[85] Allen CD, Breshears DD, McDowell NG. On underestimation of global vulnerability to tree mortality and forest die-off from hotter drought in the Anthropocene. Ecosphere 2015;6:1–55.
[86] Biederman JA, Scott RL, Goulden ML, et al. Terrestrial carbon balance in a drier world: the effects of water availability in southwestern North America. Glob Change Biol 2016;22:1867–79.
[87] Tang J, Bolstad PV, Martin JG. Soil carbon fluxes and stocks in a Great Lakes forest chronosequence. Glob Change Biol 2009;15:145–55.
[88] Thomaz SM, Agostinho AA, Gomes LC, et al. Using space-for-time substitution and time sequence approaches in invasion ecology. Freshwater Biol 2012;57:2401–10.
[89] Pickett ST. Space-for-time substitution as an alternative to long-term studies 1989 New York, NY In Long-term studies in ecology. Springer. p. 110–135.
[90] Johnson EA, Miyanishi K. Testing the assumptions of chronosequences in succession. Ecol Lett 2008;11:419–31.
[91] Wieder WR, Cleveland CC, Smith WK, et al. Future productivity and carbon storage limited by terrestrial nutrient availability. Nat Geosci 2015;8:441–4.
[92] Chen Q, Xu W, Li S, et al. Aboveground biomass and corresponding carbon sequestration ability of four major forest types in south China. Chin Sci Bull 2013;58:1551–7.
[93] Zhang L, Xiao J, Li L, et al. China's sizeable and uncertain carbon sinks: a perspectivie from GOSAT. Chin Sci Bull 2014;59:1547–55.
[94] Ma X, Wang Z. Estimation of provincial forest carbon sink capacities in Chinese mainland. Chin Sci Bull 2011;56:883–9.
[95] Zhang Y, Liang S. Changes in forest biomass and linkage to climate and forest disturbances over Northeastern China. Glob Change Biol 2014;20:2596–606.
[96] Lü A, Tian H, Liu M, et al. Spatial and temporal patterns of carbon emissions from forest fires in China from 1950 to 2000. J Geophys Res Atmos 2006;111:D05313.
[97] Wang C, Gower ST, Wang Y, et al. The influence of fire on carbon distribution and net primary production of boreal Larix gmelinii forests in north-eastern China. Glob Change Biol 2001;7:719–30.
[98] Thomas RQ, Canham CD, Weathers KC, et al. Increased tree carbon storage in response to nitrogen deposition in the US. Nat Geosci 2010;3:13–7.
[99] Nadelhoffer KJ, Emmett BA, Gundersen P, et al. Nitrogen deposition makes a minor contribution to carbon sequestration in temperate forests. Nature 1999;398:145–8.
[100] Sutton MA, Simpson D, Levy PE, et al. Uncertainties in the relationship between atmospheric nitrogen deposition and forest carbon sequestration. Glob Change Biol 2008;14:2057–63.
[101] Aber J, McDowell W, Nadelhoffer K, et al. Nitrogen saturation in temperate forest ecosystems. BioSci 1998;48:921–34.
[102] Wallace ZP, Lovett GM, Hart JE, et al. Effects of nitrogen saturation on tree growth and death in a mixed-oak forest. For Ecol Manage 2007;243:210–8.
[103] Jin W, He HS, Thompson FRIII, et al. Future forest aboveground carbon dynamics in the central United States: the importance of forest demographic processes. Sci Rep 2017;7:41821.
[104] Yue C, Ciais P, Luyssaert S, et al. Representing anthropogenic gross land use change, wood harvest, and forest age dynamics in a global vegetation model ORCHIDEE-MICT v8.4.2. Geosci Model Dev 2018;11:409–28.

Yitong Yao received her B.S. degree from Beijing Forestry University, China in 2015, and now is a master student in College of Urban and Environmental Sciences, Peking University, China. Her current research interest is mainly focused on the application of machine learning algorithms in estimating forest carbon fluxes and understanding responses of forest productivity to climate change and soil nutrient availability.

Shilong Piao is Cheung Kong Professor of Peking University. His current research focuses on the data-model integration to improve our ability for predicting terrestrial ecosystem responses to global change.